Atmospheric
Chemistry
and Physics

Ozone and NO_x chemistry in the eastern US: evaluation of CMAQ/CB05 with satellite (OMI) data

T. P. Canty[1], L. Hembeck[1], T. P. Vinciguerra[1], D. C. Anderson[1], D. L. Goldberg[1], S. F. Carpenter[1], D. J. Allen[1], C. P. Loughner[2,3], R. J. Salawitch[1,2,4], and R. R. Dickerson[1]

[1]Department of Atmospheric and Oceanic Science, University of Maryland, College Park, MD, USA
[2]Earth System Science Interdisciplinary Center, University of Maryland, College Park, MD, USA
[3]NASA Goddard Space Flight Center, Greenbelt, MD, USA
[4]Department of Chemistry and Biochemistry, University of Maryland, College Park, MD, USA

Correspondence to: T. P. Canty (tcanty@atmos.umd.edu)

Abstract. Regulatory air quality models, such as the Community Multiscale Air Quality model (CMAQ), are used by federal and state agencies to guide policy decisions that determine how to best achieve adherence with National Ambient Air Quality Standards for surface ozone. We use observations of ozone and its important precursor NO_2 to test the representation of the photochemistry and emission of ozone precursors within CMAQ. Observations of tropospheric column NO_2 from the Ozone Monitoring Instrument (OMI), retrieved by two independent groups, show that the model overestimates urban NO_2 and underestimates rural NO_2 under all conditions examined for July and August 2011 in the US Northeast. The overestimate of the urban to rural ratio of tropospheric column NO_2 for this baseline run of CMAQ (CB05 mechanism, mobile NO_x emissions from the National Emissions Inventory; isoprene emissions from MEGAN v2.04) suggests this model may underestimate the importance of interstate transport of NO_x. This CMAQ simulation leads to a considerable overestimate of the 2-month average of 8 h daily maximum surface ozone in the US Northeast, as well as an overestimate of 8 h ozone at AQS sites during days when the state of Maryland experienced NAAQS exceedances. We have implemented three changes within CMAQ motivated by OMI NO_2 as well as aircraft observations obtained in July 2011 during the NASA DISCOVER-AQ campaign: (a) the modeled lifetime of organic nitrates within CB05 has been reduced by a factor of 10, (b) emissions of NO_x from mobile sources has been reduced by a factor of 2, and (c) isoprene emissions have been reduced by using MEGAN v2.10 rather than v2.04. Compared to the baseline simulation, the CMAQ run using all three of these changes leads to considerably better simulation of column NO_2 in both urban and rural areas, better agreement with the 2-month average of daily 8 h maximum ozone in the US Northeast, fewer number of false positives of an ozone exceedance throughout the domain, as well as an unbiased simulation of surface ozone at ground-based AQS sites in Maryland that experienced an ozone exceedance during July and August 2007. These modifications to CMAQ may provide a framework for use in studies focused on achieving future adherence to specific air quality standards for surface ozone by reducing emission of NO_x from various anthropogenic sectors.

1 Introduction

The spatial scale of tropospheric ozone production is of enormous consequence, especially for the eastern US where cross-state transport of air pollutants is a major policy concern (EPA vs. EME, 2014). As early as the 1980's (Logan, 1989), analysis of measurements indicated that surface ozone episodes covered areas approaching $10^6\ km^2$. Numerous observational studies have demonstrated the westerly transport of ozone and its precursors and the impact of upwind emissions that lead to high concentrations of surface ozone in the eastern United States (Brent et al., 2013; Hains et al., 2008; He et al., 2014, 2013a, b; Ryan et al., 1998; Taubman et al., 2004, 2006). Dramatic improvements in air quality have been

observed due to reductions in the emission of ozone precursors (Butler et al., 2011; Fiore et al., 1998; Gego et al., 2007; He et al., 2013b; Marufu et al., 2004; Walsh et al., 2008). Numerical simulations of ozone show a dependence on NO$_x$ (NO + NO$_2$) concentrations, but do not always capture the regional nature of photochemical smog events nor the strength of the response to NO$_x$ emission controls (Fujita et al., 2013; Gilliland et al., 2008; Godowitch et al., 2008a, b; Hogrefe et al., 2011; Pollack et al., 2013; Wilson et al., 2012; Yegorova et al., 2011; Zhou et al., 2013). Recognizing that long-range transport affects local compliance of federally mandated standards, the EPA enacted the Cross State Air Pollution Rule (CSAPR) http://www.epa.gov/crossstaterule which reduces the emissions of ozone precursors from power plants. Phase 1 of the CSAPR emissions budgets is scheduled for implementation in 2015.

The Community Multiscale Air Quality model (CMAQ) is used extensively for regulatory purposes (Byun and Schere, 2006). State Implementation Plans (SIPs) quantify future emission reductions that will bring nonattainment areas into compliance with the National Ambient Air Quality Standard (NAAQS) for surface ozone. The recommendations submitted in the SIPs are based on analysis of output from air quality models such as CMAQ that simulate meteorology and the nonlinearities inherent in tropospheric ozone chemistry. Oxides of nitrogen play a controlling role in ozone production in the eastern US and comparison of monitor records with CMAQ output suggests that this model overestimates NO$_x$ concentrations in urban areas, but underestimates NO$_x$ in rural areas (Castellanos et al., 2011). The overestimate of NO$_x$ in urban areas, coupled with the underestimate in rural areas, means CMAQ may keep NO$_x$ too closely confined to source regions, thereby underestimating the interstate transport of ozone precursors. Such disagreement may stem from the complicated nature of NO$_x$ emissions, recycling, and removal though proper representation of dynamics (e.g. vertical mixing) may also play a role. Organo-nitrate compounds can act as reservoirs or sinks for NO$_x$ and have received substantial attention for many years (Atlas, 1988; Beaver et al., 2012; Day et al., 2003; Farmer et al., 2006; Lockwood et al., 2010; Neff et al., 2002; Perring et al., 2013, 2010, 2009; Xie et al., 2013). The production and loss mechanisms that govern the concentrations of organo-nitrate species are largely simplified in most air quality models. Ground-based and aircraft measurements of ozone and its precursors provide important constraints on the concentrations of trace gasses and can be used to validate model output. However, these data are geographically limited. In contrast, satellites provide a measure of the spatial variation of these species over a much larger domain. In this study, we investigate the regional representation of NO$_2$ in CMAQ by comparing model output to satellite observations from the Ozone Monitoring Instrument (OMI) (e.g., Boersma et al., 2011; Bucsela et al., 2013) during July and August 2007. Modifications to the chemical mechanism and emissions inventories used by the model

are suggested to improve agreement between model and observations. More relevant to policy makers is the ability of air quality models to reproduce surface ozone. We extend our analysis to include comparisons between model output and ozone observed at ground-based stations. The model domain for this study is the eastern United States (i.e., most of the states eastward of the Mississippi river), a region that has been the focus of intense SIP modeling efforts by mid-Atlantic states and for which detailed emissions inventories and meteorological fields are readily available.

2 Data description: OMI satellite

OMI is one of four instruments onboard the NASA Aura satellite, now in its tenth year http://aura.gsfc.nasa.gov/. The satellite is in a sun synchronous orbit, providing OMI with a daytime overpass at ∼ 13:40 local time (LT). NO$_2$ columns are retrieved using differential optical absorption spectroscopy (DOAS) in the 405–465 nm range. There are two operational retrievals of tropospheric column NO$_2$ based on radiances measured by OMI; the Derivation of OMI tropospheric NO$_2$ (DOMINO) product (Boersma et al., 2007, 2011) provided by the Royal Netherlands Meteorological Institute (KNMI) and the NASA Goddard Space Flight Center (GSFC) product (Bucsela et al., 2013).

Retrievals of tropospheric column NO$_2$ (hereafter, column NO$_2$) from OMI are available for the width of the atmosphere observed along the viewing track (or swath) of the instrument. OMI tropospheric column NO$_2$ is calculated by subtracting the stratospheric signal from the observations of total column NO$_2$. The method of determining the stratospheric component varies between the GSFC and DOMINO product and is explained in Bucsela et al. (2013) and Boersma et al. (2007), respectively. GSFC assumes that total column NO$_2$ over regions with little expected tropospheric influence represents the stratospheric column. This field of stratospheric column NO$_2$ is interpolated over nearby regions of high surface pollution and removed from the total column NO$_2$ retrieval to determine tropospheric column NO$_2$. For the DOMINO product, data assimilation of OMI slant columns with the TM4 model (Tracer Model version 4, van Noije et al., 2006) determines the stratospheric subtraction. These level 2 (L2) observations do not occur on a regularly spaced grid. For a more meaningful comparison between satellite retrievals and model output, we generate level 3 (L3) products on a 0.25° × 0.25° (latitude, longitude) grid for both observed and calculated column NO$_2$. Column NO$_2$ from OMI is weighted based on satellite viewing angle using the formulation of Bucsela et al. (2013). These same weights are applied to column NO$_2$ from CMAQ to assure a meaningful comparison.

Column NO$_2$ measurements are only considered for the gridding procedure when solar zenith angle is less than 85° and effective cloud fraction (Acarreta et al., 2004) is

less than 30 %. Observations are only considered valid and used for our analysis if the flag "xtrackqualityflag", provided in the data files for both retrievals, is equal to zero. This flag indicates which OMI data products can be used in a manner that minimizes the influence of the row anomaly along the observing swath (see http://www.knmi.nl/omi/research/product/rowanomaly-background.php for more information). Summary quality flags, also provided in the data files, provide quality assurance that at least 50 % of the tropospheric column is determined by observed information. In our study, retrievals are only used when this flag also equals zero. Comparison with model output is facilitated through the use of averaging kernels (DOMINO) or scattering weights (GSFC). No uncertainties are provided explicitly for the averaging kernels or scattering weights. Instead, the DOMINO retrieval team provides uncertainties ("VCDTropErrorUsingAVKernel") that account for errors in both the NO_2 column and the averaging kernel. The precision in the GSFC NO_2 product is provided in the variable "ColumnAmountNO2TropStd". We use these uncertainties as the defacto way of comparing the two different retrievals of column NO_2 to model output of this quantity.

The production of ozone in our region of study is NO_x-limited for nearly all of the domain. An analysis of satellite observations acquired in 2005 to 2007 shows that ozone production is VOC-limited for only a small part of New York City, with the rest of the domain being NO_x-limited (Duncan et al., 2010). Hence, the general focus of this manuscript is on model representation of nitrogen oxides. The results of this study may not be applicable to regions where production of ozone is VOC dominant, which occurs primarily in rural regions such as the so-called isoprene volcano of the Ozarks (Carlton and Baker, 2011) or regions of intense hydrocarbon processing such as Houston, Texas (Li et al., 2007).

3 Model description

For this analysis we use the Community Multiscale Air Quality (CMAQ) modeling system version 4.7.1 (https://www.cmascenter.org/cmaq/). This model has been used extensively by states that are members of the Ozone Transport Commission (OTC) in preparation for the 2015 ozone SIP call. For this analysis, CMAQ simulations were performed for the Eastern US with a $12 \, km \times 12 \, km$ horizontal resolution and a 34 layer (σ coordinate) vertical grid from the surface to $\sim 20 \, km$ with hourly output. CMAQ does not include stratospheric processes so the upper layers of the model atmosphere should not be used for research purposes. The analysis presented here is limited to altitudes below the tropopause. Simulated meteorology is driven by output from the Weather Research Forecasting (WRF v3.1.1) model for year 2007 and processed for use in CMAQ by the Meteorological Chemistry Interface Processor (MCIP).

Emissions inventories for year 2007 were developed by the Mid-Atlantic Regional Air Management Association, Inc. (MARAMA) specifically for use in OTC modeling efforts. Biogenic emissions were estimated using the Model of Emissions of Gases and Aerosols in Nature (MEGAN v2.04) (Guenther et al., 2006). Emissions from on-road mobile sources were developed using the Motor Vehicle Emission Simulator (MOVES) (USEPA, 2010) while off–road emissions were supplied by the National Mobile Inventory Model (NMIM) (USEPA, 2005). Emissions due to aircraft are included in the inventories based on take-off and landing data for individual airports. Emission inventories and WRF/MCIP meteorology are merged and gridded using the Sparse Matrix Operator Kernel Emissions (SMOKE v3.1, https://www.cmascenter.org/smoke/) model to generate time-varying, three dimensional CMAQ ready emission fields. CMAQv4.7.1 uses the 2005 Carbon Bond (CB05) chemical mechanism (Yarwood et al., 2005). Though there is a more recent version of the Carbon Bond chemical mechanism (CB6) it is not available for use in publicly available versions of CMAQ as of the submission of this manuscript.

We have added lightning-generated NO_x (L_{NO_x}), assuming an NO_x production rate of $500 \, moles \, flash^{-1}$, to the merged emissions files following the parameterization described in Allen et al. (2012). The production of L_{NO_x} is correlated to lightning flashes observed by the National Lightning Detection network (NLDN), which records cloud to ground flashes (CG). The amount of intercloud lightning (IC) is calculated based on a climatological IC / CG ratio (Boccippio et al., 2001). In general, the amount of NO_x supplied by lightning is much smaller than anthropogenic sources, especially in urban areas. This may not necessarily be true in the future as further pollution control measures are enacted to reduce the emissions of NO_x from power plants, vehicles, etc. Neglecting L_{NO_x} may result in modeled NO_x being biased low, especially in rural regions where NO_x levels are already much lower than in urban regions.

Modeled tropospheric column NO_2 is calculated by integrating the CMAQ NO_2 profiles from the surface to the level of the tropopause provided by either the DOMINO or GSFC retrieval teams. Model output at the hour closest to the OMI overpass time are convolved with the air mass factors and averaging kernels (DOMINO) or scattering weights (GSFC) appropriate for the two satellite retrievals. We interpolate the CMAQ output to the pressure grid of the averaging kernel/scattering weight. The DOMINO tropospheric averaging kernel is calculated by taking the product of the averaging kernel and the ratio of the air mass factor to the tropospheric air mass factor (Boersma et al., 2011). CMAQ output is multiplied by the tropospheric averaging kernel and then integrated over pressure. In a similar fashion, GSFC scattering weights are applied to the model profiles of NO_2 to generate CMAQ tropospheric column NO_2 for direct comparison with the GSFC tropospheric NO_2 product (Bucsela et al., 2013; Lamsal et al., 2014).
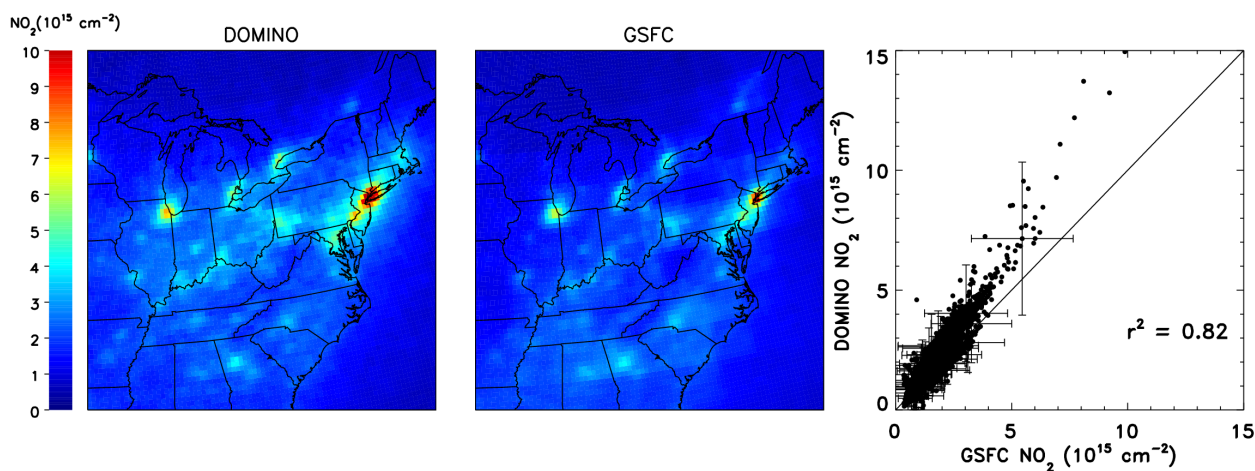
Figure 1. Average OMI tropospheric column NO_2 observations for July and August 2007 for both the DOMINO (left) and GSFC (middle) retrievals. The level 2 swath data for both retrievals have been screened, weighted based on viewing angle and gridded onto a $0.25° \times 0.25°$ lat/lon grid. Only observations where cloud fraction is less than 30 % are used in the gridding process. Both data sets indicate that the highest levels of tropospheric NO_2 occur over urban regions. A scatter plot of DOMINO vs. GSFC observations (right) indicates that the DOMINO retrieval is roughly 20 % higher, on average, than the GSFC satellite product. Error bars indicate the uncertainty in the satellite retrievals.

Only those model grid points closest to the center of each pixel along the satellite swath are considered. To generate a model L3 gridded product, CMAQ output at each model grid cell is only used if the co-located satellite retrieval satisfies the quality flags and cloud fraction limits described above (i.e., we only use those CMAQ points where the closest satellite retrieval is also considered "valid"). CMAQ output is screened and gridded in an identical fashion as the respective OMI retrievals, to generate model L3 products (one for the DOMINO retrieval, the other for the GSFC retrieval) appropriate for comparison to the satellite data.

4   Analysis and results

4.1   Model/satellite comparisons

Gridded, L3 satellite retrievals of tropospheric column NO_2 over the Eastern US for the July/August 2007 period of study are shown in Fig. 1. Both the DOMINO and GSFC retrievals exhibit similar patterns of elevated NO_2 over urban centers and lower, but substantial and quantifiable NO_2 in rural regions. The two retrieval products are well correlated ($r^2 = 0.82$) and generally fall within the error bars of the observations. Column NO_2 found by the DOMINO retrieval is ~ 20 % higher than column NO_2 found using the GSFC retrieval. It is beyond the scope of this paper to probe the cause of this disagreement. As such, we will compare both satellite retrievals to model output separately. This difference between data sets may affect attempts to estimate emissions of NO_x from satellite retrievals. Our focus is on the *ratio* of column NO_2 between urban and rural regions; both retrievals yield similar scientific conclusions.

Figure 2 shows comparisons of the baseline CMAQ model ($CMAQ_{BSE}$) value of column NO_2 to the satellite data product found by both retrievals. Regions of elevated column NO_2 are calculated over urban regions, roughly similar to observation, but the modeled column NO_2 is significantly smaller over rural areas than reported by OMI. The correlation between model and observed NO_2, shown for both retrievals in Fig. 2, is largely driven by the high density of points where column NO_2 is below 5×10^{15} cm^{-2} (Fig. 2, right panels). In this region of the distribution, observed NO_2 is larger than the baseline air quality model for both satellite retrievals. The mean ratio of model to observations across the domain, which is predominantly rural, is 0.34 and 0.37 for DOMINO and GSFC, respectively. In the predominantly urban regions (red points, right panels of Fig. 2) the opposite is true; the mean ratio of model to observed NO_2 rises to 1.56 and 1.62 for the two retrievals.

To highlight areas where the model is higher than observations we restrict our maps to only show those places where model calculations are at least 25 % higher than observed by satellite (Fig. 3). The regions that meet the 25 % criteria are generally large urban centers for which CMAQ NO_2 is usually biased high by 50 to 60 % (DOMINO and GSFC retrievals, respectively). This overestimate of column NO_2 is not true for all highly populated urban centers, such as the I-95 corridor from Washington, DC through Philadelphia, PA. Over the entire domain shown in Fig. 2, NO_2 found using $CMAQ_{BSE}$ is ~ 60 % lower than observed. Overall, the ratio of urban NO_2 (those areas shown in Fig. 3) to rural NO_2 (all other areas) in the model is at least a factor of 2 larger than the same ratio calculated from space-based observations. Calculations of reduced chi squared, χ^2, for these urban regions (GSFC $= 1.69$, DOMINO $= 1.4$) indicates that
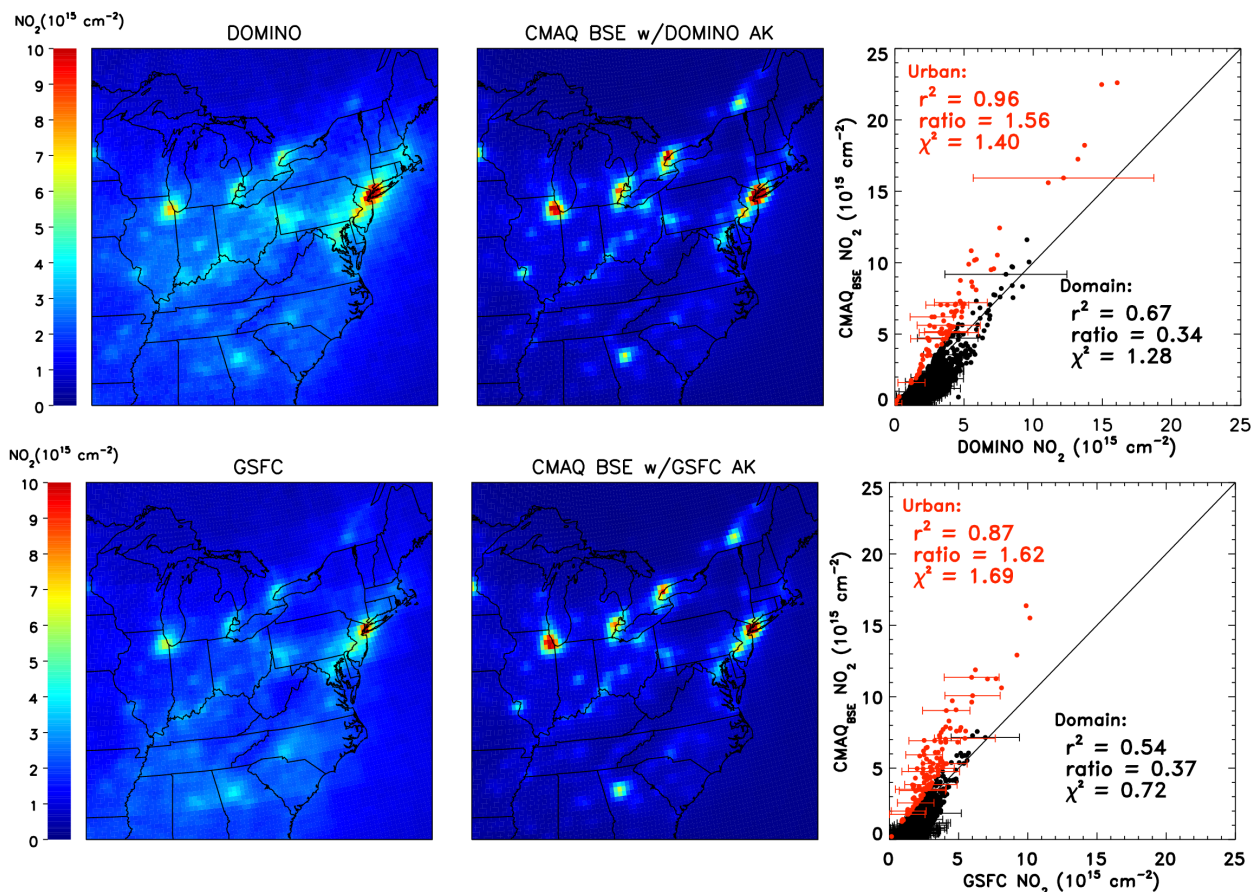
Figure 2. Comparison of satellite observations of tropospheric column NO$_2$ (left panels) to output from a baseline CMAQ model run (CMAQ$_{BSE}$) convolved with the satellite-averaging kernels for the DOMINO retrieval (top middle) and GSFC retrieval (bottom middle). Model output is screened, weighted, and gridded in the same manner as the satellite retrievals. Scatter plots of model and satellite NO$_2$ provide a more quantitative comparison (right panels). Error bars represent the uncertainty in the satellite retrievals. Metrics are provided to test the level of agreement between model and observations. The variance (r^2), reduced chi-squared (χ^2), and the mean ratio are calculated for all points within the model domain (black points). r^2 indicates the model can explain ∼ 50–70 % of the satellite observations. The relatively low value of the mean ratio is driven by the large concentration of points below 5×10^{15} cm^{-2}, where the model underpredicts the satellite. χ^2 is better for the GSFC retrieval (0.72) than for DOMINO (1.28). The same metrics are calculated for grid cells where the simulations are at least 25 % greater than observations (called "Urban", red points). While the variance is good, the ratio is high and χ^2 implies that baseline modeled tropospheric column NO$_2$ falls outside the uncertainties of the observations.

the elevated modeled column NO$_2$ can not be reconciled with the observations using the uncertainty estimates in the satellite retrievals. These results agree with reported discrepancies based on comparison of CMAQ output to observations of column NO$_2$ from SCIAMACHY (Napelenok et al., 2008) as well as surface NO$_2$ (Castellanos, 2009). Use of the BEHR (Russell et al., 2011) retrieval of column NO$_2$ (not shown) gives similar results. Table 1 summarizes the numerical comparisons between the DOMINO satellite retrievals and all model simulations presented in this study. Table 2 shows similar comparisons but for the GSFC retrieval. In a recent study, Lamsal et al. (2014) compared OMI NO$_2$ to in situ and surface observations and reported OMI retrievals may be lower than observations in urban regions and higher in rural

regions, on the order of 20 %. This is the opposite of our results, however, the OMI/observation biases are not enough to explain the model/OMI disagreement presented here.

4.2 Long-lived NO$_x$ precursors

The CB05 chemical mechanism represents all organic nitrate species, such as alkyl nitrates (e.g., isopropyl nitrate, n-propyl nitrate, isobutyl nitrate, isoprene nitrates), as a single species called NTR (Yarwood et al., 2005). In CB05, NTR is created by the breakdown of isoprene and isoprene products such as methacrolein (MACR) and methyl vinyl ketone (MVK) and is lost through photolytic and oxidation processes. The photolysis of NTR is calculated in the model using the cross section of isopropyl nitrate to represent all or-
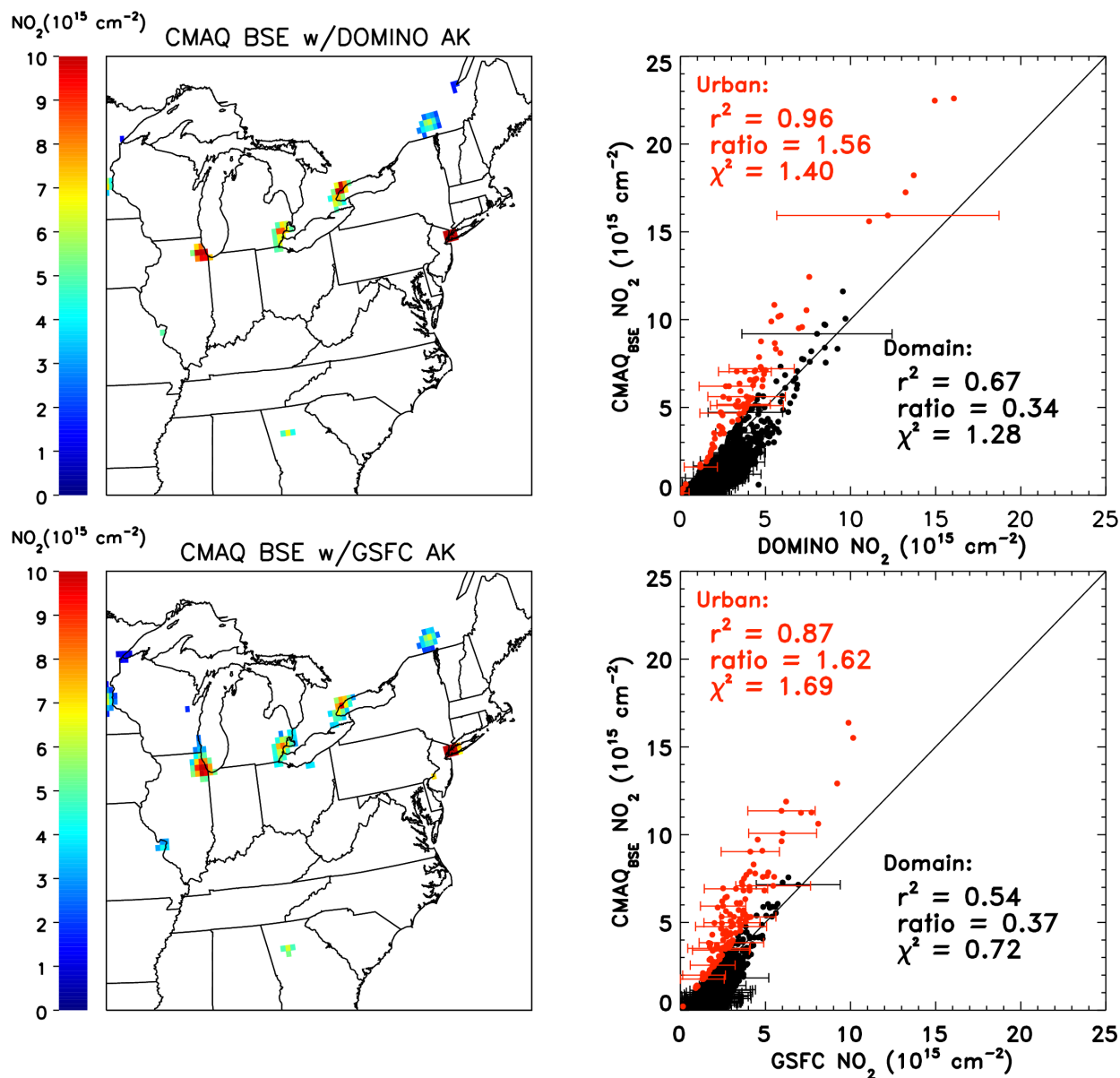
Figure 3. The same model output as Fig. 2 except results are only shown for regions where the simulations are at least 25 % greater than observations (left panels). This clearly shows that model is biased high over urban regions indicated by the red points in the scatter plots (right panels).

ganic nitrate species and produces NO$_2$ and HO$_2$, important precursors to surface O$_3$ formation (Yu et al., 2010).

We have diagnosed the lifetime of NTR due to photolysis to be ~ 10 days in CMAQ during summer, in agreement with the lifetime of C$_2$ to C$_4$ alkyl nitrates in the mixed layer (Luke et al., 1989). The CMAQ lifetime for NTR is based on photolysis frequencies calculated by the photolysis rates preprocessor module (jproc). Within CMAQ, NTR often constitutes 20 to 40 % of the total NO$_y$ budget. The long lifetime of NTR results in sequestration of nitrogen compounds far from the emission source, perhaps accounting for the low pre-

dicted values of CMAQ NO$_2$ in rural areas. Analysis of aircraft observations, however, indicates the speciation of NTR is not well described in CMAQ using CB05, with the most abundant species in this family being hydroxynitrates with lifetimes on order ~ 1 day or less (Horowitz et al., 2007; Perring et al., 2009; Beaver et al., 2012). Furthermore, a recent analysis of laboratory studies that evaluated absorption cross sections and photolysis frequencies indicates that the photolysis of carbonyl nitrates may be 3 and 20 times faster than previously reported (Müller et al., 2014).
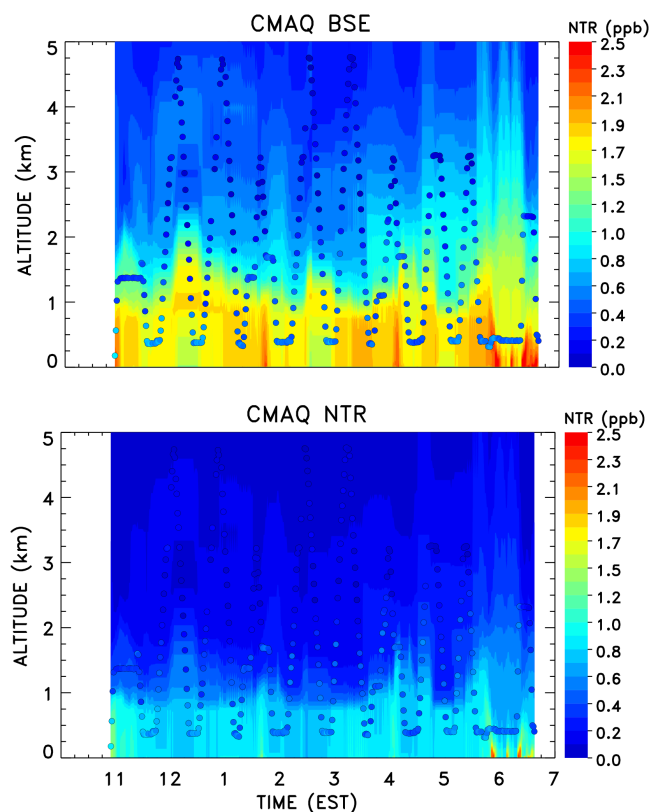
Table 1. Values of the variance (r^2), mean ratio, and reduced chi-squared (χ^2) calculated for all model simulations compared to the DOMINO retrievals of tropospheric column NO$_2$.

	Model simulation				
	BSE	NTR	MGN	N50	TOT
Domain:					
r^2	0.67	0.71	0.71	0.73	0.78
Ratio	0.34	0.40	0.34	0.56	0.55
χ^2	1.28	1.04	1.21	0.67	0.63
Urban:					
r^2	0.96	0.96	0.91	0.96	0.92
Ratio	1.56	1.60	1.21	1.75	1.39
χ^2	1.40	1.50	0.28	2.15	0.55

Table 2. Values of the variance (r^2), mean ratio, and reduced chi-squared (χ^2) calculated for all model simulations compared to the GSFC retrievals of tropospheric column NO$_2$.

	Model simulation				
	BSE	NTR	MGN	N50	TOT
Domain:					
r^2	0.54	0.60	0.59	0.58	0.64
Ratio	0.37	0.44	0.38	0.62	0.60
χ^2	0.72	0.59	0.66	0.42	0.37
Urban:					
r^2	0.87	0.88	0.81	0.90	0.83
Ratio	1.62	1.65	1.24	1.80	1.41
χ^2	1.69	1.80	0.39	2.44	0.68

Figure 4. (Top panel) Comparison of baseline CMAQ simulations of organic nitrates (NTR) (colored contours) to NTR observed during the DISCOVER–AQ field mission on 29 July 2011 (colored points). (Bottom panel) As in the top panel, except the CB05 chemical mechanism in CMAQ has been modified such that the lifetime of NTR is reduced by a factor of 10.

A comparison of NTR from a baseline CMAQ run to measurements obtained during the 2011 NASA DISCOVER-AQ field mission shows modeled NTR to be 2–4 times greater than observed (Fig. 4, top). This version of the model uses emissions inventories and meteorological fields appropriate for 2011 (Loughner et al., 2011; Anderson et al., 2014; Goldberg et al., 2014; Flynn et al., 2014; He et al., 2014). To investigate the source of this discrepancy we have increased the photolysis frequency of NTR by a factor of 10, reducing the lifetime to $\sim$ 1 day. This model scenario will be referred to as CMAQ$_{NTR}$ for the remainder of this study. Values of NTR found using a shorter lifetime are in much better agreement with observed NTR, indicating a significant improvement in the model representation of alkyl nitrate chemistry (Fig. 4, bottom). We recognize that decreasing the lifetime of NTR with respect to photolysis by a factor of 10 may be too simplistic, but this calculation is meant to illustrate how a thorough representation of the NTR family of gasses may lead to overall improvements to the model framework. A full revision of alkyl nitrate is being undertaken by the EPA (Leucken and Schwede, 2014).

The breakdown of NTR, having a lifetime of $\sim$ 1 day, increases local NO$_2$ both by direct production of NO$_2$ and by shifting the partitioning of NO$_x$ toward NO$_2$ via the HO$_2$ + NO reaction. A comparison of CMAQ tropospheric column NO$_2$ (convolved with the averaging kernels) found for the CMAQ$_{NTR}$ simulation and OMI column NO$_2$ is shown in Fig. 5. There is slightly better agreement between modeled and column NO$_2$ and both satellite retrievals for the entire domain compared to the baseline simulation, generally due to increased NO$_2$ in rural areas for CMAQ$_{NTR}$. However, for CMAQ$_{NTR}$, modeled column NO$_2$ in urban regions (red points, Fig. 5) lies further from observed NO$_2$ than found for the baseline simulations.

In CB05, 100 % of the NO$_x$ from photolysis of NTR or its products is recycled. Loss through OH attack, also fast for isoprene nitrates, yields HNO$_3$, a NO$_x$ sink in the troposphere. The model output presented here can be considered a bounding scenario since this treatment of NO$_x$ is an oversimplification. If NO$_x$ recycling were not 100 % efficient, we would expect a decrease in column NO$_2$ throughout the domain, and a corresponding reduction in O$_3$. It is beyond the
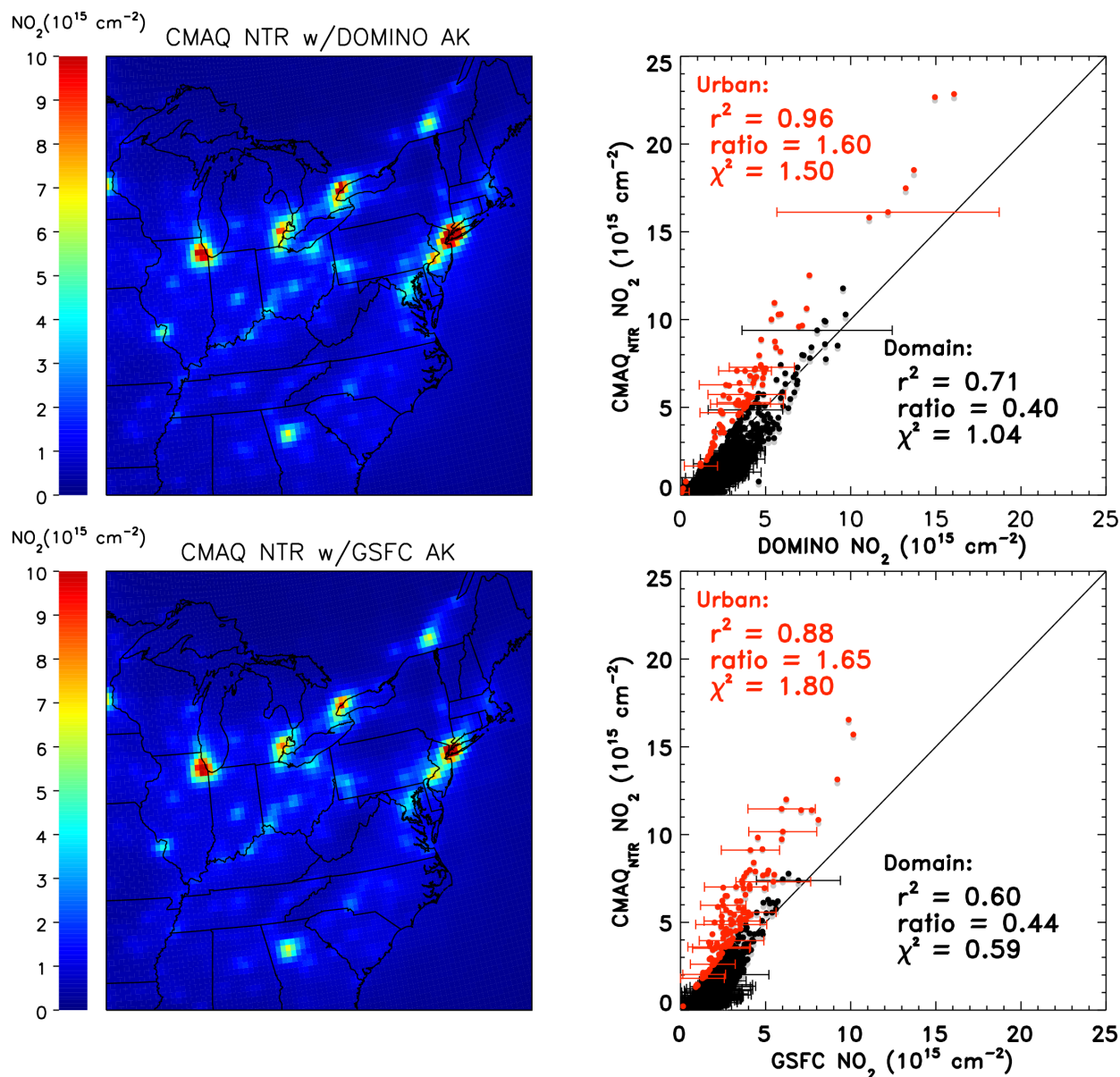
Figure 5. Similar to Fig. 2 except the chemical mechanism in the CMAQ model has been modified such that the lifetime of NTR is reduced by a factor of 10 ($CMAQ_{NTR}$). Gray points on the scatter plots represent the results shown in Fig. 2 (right panels). As in Fig. 3, red points represent urban regions.

scope of this study to assess the sensitivity of NO_2 and O_3 to this level of detail of the CB05 mechanism.

Emissions from airplanes en route are not considered in the emissions inventories. However, the overall contribution from aircraft aloft to the tropospheric column is relatively minor (i.e., less than 1 % of tropospheric column) and would not explain the urban / rural discrepancy between satellite observations and model output (Jacobson et al., 2013).

4.3 Emissions of NO_x from mobile sources

A comparison of NO_x from emission inventories for 2011 to observations taken during DISCOVER-AQ (July 2011) has quantified a potential overestimation of mobile NO_x (Anderson et al., 2014). The ratio of CO / NO_y from observations was roughly a factor of 2 greater than the ratio based on the National Emissions Inventory data used in CMAQ. Model CO is only $\sim 15\%$ greater than observed for this time period, indicative of a large overestimate of mobile NO_x emissions (Anderson et al., 2014). This conclusion is in agreement with

a study by Yu et al. (2012) who compared CMAQ simulations, using the CB4.2 chemical mechanism, to aircraft data acquired during the TexAQS/GoMACCS campaign. National Emissions Inventory (NEI) point and area sources for year 2001 were projected to 2006 and mobile emissions were generated from the EPA MOBILE6 model. Yu et al. (2012) report modeled CO $\sim 10\%$ greater than measured. However, the ratio of observed $CO/NO_y = 26.9$ (determined using values from Table 4, Yu et al., 2012) is roughly a factor of 2 higher than the CMAQ calculated ratio of $CO/NO_y = 13.1$. A separate analysis of 2011 DISCOVER-AQ observations has shown that CMAQ consistently overestimated NO_y by a factor of 2 from the surface to 3000 m altitude (Goldberg et al., 2014).

Airborne observations analogous to those taken during DISCOVER-AQ in summer 2011 do not exist for summer 2007. We have examined observations of CO and NO_x from six surface air quality monitoring sites in Maryland, Northern Virginia, and the District of Columbia acquired during summer 2007. The chemiluminescence method of detecting NO_x suffers from known interferences (Castellanos et al., 2011; Dunlea et al., 2007; Fehsenfeld et al., 1987). It is reasonable to assume that the surface sites are actually reporting $NO_x^* = NO_y - HNO_3$. For the summer of 2007, CO observations also seem to have calibration issues. Nonetheless, we have compared the observed ratio of CO/NO_x^* from these six sites to the CMAQ value of CO/NO_x^*, where CMAQ is sampled at the time and location of each surface observation. The mean and 1σ standard deviation of the observed divided by modeled value of CO/NO_x^* is 1.97 ± 1.5 for summer 2007; the large SD reflects a great deal of noise in the surface observations. The fact that observed CO/NO_x^* exceeds the modeled value of this quantity supports the notion that mobile emissions in the 2007 inventory exceed the actual emissions from this source by an amount comparable to that reported by Anderson et al. (2014). Doraiswamy et al. (2009) also report a possible over-prediction in area source emissions.

Following Anderson et al. (2014), we assume that there is a similar overestimation of NO_x in the 2007 emissions inventories used in our analysis and we test for this discrepancy by reducing on-road mobile NO_x emissions by a factor of 2. Results from a CMAQ model run that considers this change as well as the reduction in NTR lifetime in the CB05 chemical mechanism, termed $CMAQ_{N50}$ (i.e., a factor of 2 or 50% reduction), are shown in Fig. 6. The most noticeable difference between these results and those presented in Figs. 2 and 5 is the reduction in column NO_2 over urban regions, which is now in much better agreement with satellite observations (ratios between model and observations of 1.21 and 1.24 for DOMINO and GSFC, respectively). While the modifications to the CB05 chemical mechanism and emissions inventories have somewhat reconciled the differences between modeled and remotely sensed urban tropospheric column NO_2, rural NO_2 is still underestimated by the model. Mean ratios for

the domain (0.34 and 0.38) are similar to results from the baseline model. Essentially, these modifications to the model have improved the urban disagreement, but overall model performance is unchanged.

4.4 Biogenic emissions

As stated above, the original emissions inventories generated by MARAMA include biogenic sources from the Model of Emissions of Gases and Aerosols in Nature (MEGAN v2.04) (Guenther et al., 2006). Since the 2007 emissions inventories were made available, an updated version of MEGAN was released (v2.10, Guenther et al., 2012). One of the main differences in biogenic emissions between the two versions of MEGAN is that isoprene, the dominant VOC in the mid-Atlantic region, has decreased by about 25% in the latest version. Emissions of biogenic isoprene calculated using MEGAN v2.10 are significantly less sensitive to high levels of photochemically active radiation (PAR) compared to earlier versions of MEGAN, resulting in lower isoprene during midday near the time of OMI overpass. An in-depth analysis of the sensitivity of regulatory air quality models to simulation of biogenic emissions will be the subject of a forthcoming paper.

Fundamentally, isoprene oxidation is initiated by reaction with OH to generate isoprene peroxy radical intermediates, termed RO_2. In the presence of NO_x, these RO_2 intermediates react with NO, producing MVK, MACR, HCHO, and a small amount of organic nitrates (Paulot et al., 2009). Overall, when output from the latest version of MEGAN is incorporated into the emissions inventories ($CMAQ_{MGN}$) there is an overall increase in column NO_2 across the model domain due to the reduction in NO_x sinks (Fig. 7).

Combining the modifications to the CB05 chemical mechanism with the changes to mobile and biogenic emissions yields the best overall agreement between model and observations ($CMAQ_{TOT}$, Fig. 8) over the model domain. The correlation between measured and modeled NO_2 is larger for $CMAQ_{TOT}$ ($r^2 = 0.78$, 0.64 for DOMINO, GSFC) than for any other model scenario. Modeled NO_2 for urban regions is in even better agreement with the satellite retrievals for all of the calculated metrics. While further work is needed, we have succeeded in decreasing the urban overestimate and rural underestimate of tropospheric column NO_2 compared to satellite data by: (a) using the latest version of MEGAN, (b) prescribing a factor of 2 reduction in mobile NO_x emissions throughout the domain, and (c) reducing the lifetime of NTR within CB05 by a factor of 10.

5 Model uncertainties

There are other possible sources of error within the model framework. Updates to the kinetics based on recent studies may affect the loss of NO_2. Mollner et al. (2010) report the
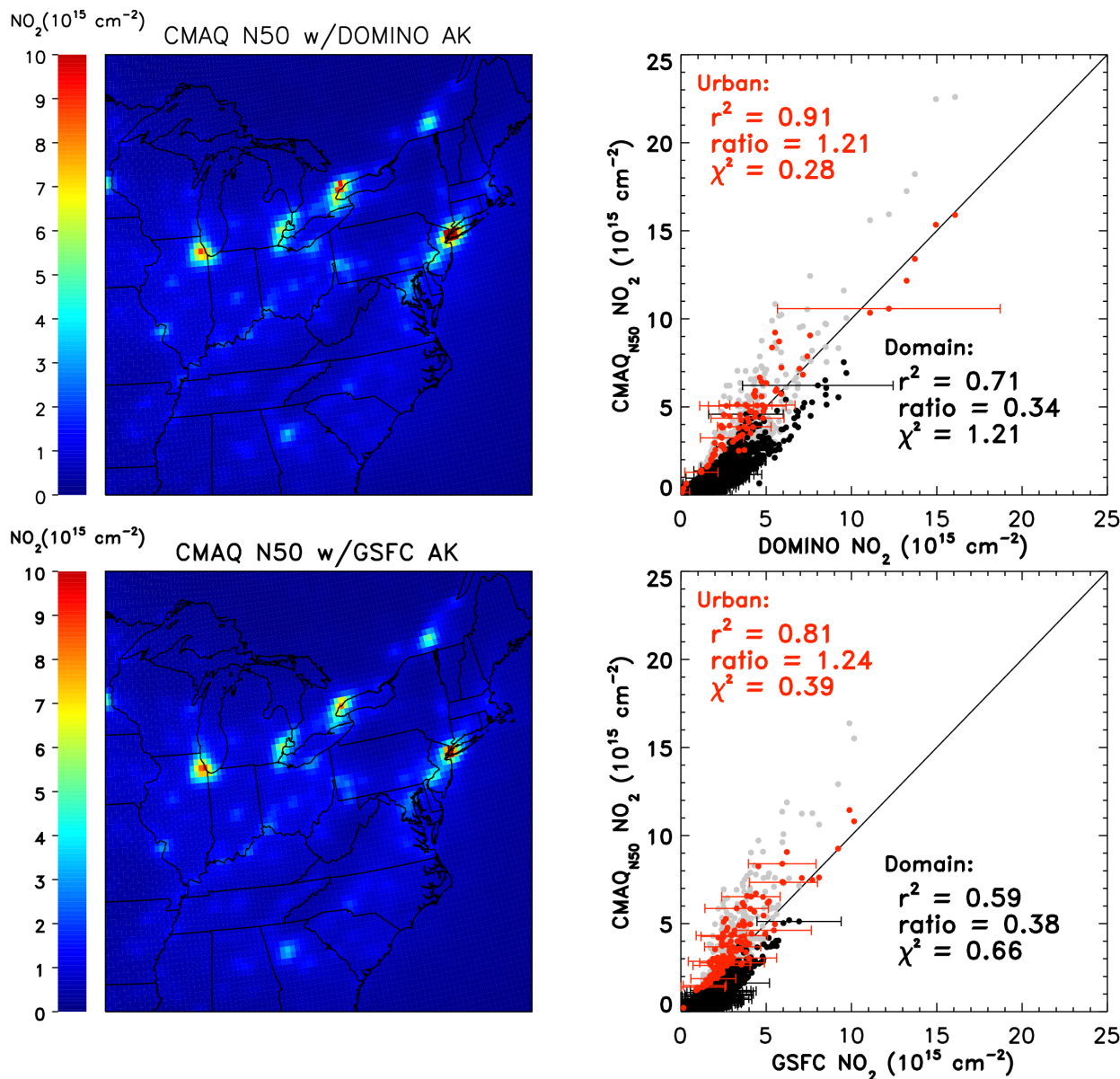
Figure 6. Same as Fig. 2 except model results include both changes to NTR chemistry and a 50 % reduction in the emissions of NO_x from mobile sources ($CMAQ_{N50}$). Gray points on the scatter plots represent the results shown in Fig. 2 (right panels).

reaction rate of $OH + NO_2 + M$ is slower than what has been recommended by prior work (Atksinson et al., 2004; Sander et al., 2006). The uptake of N_2O_5 in aerosols is likely overestimated in models (Han et al., 2015; Stavrakou et al., 2013; Vinken et al., 2014; Yegorova et al., 2011). We have performed two model simulations that consider the slower reaction rate of $OH + NO_2 + M$ ($CMAQ_{OH+NO_2}$) and assume the heterogeneous removal of N_2O_5 is zero ($CMAQ_{N_2O_5}$). Both of these scenarios also include all of the changes made to the model framework in $CMAQ_{TOT}$. Results are presented in the Supplement. Overall, both of these changes to the model show very little difference for column NO_2 compared to that

found in $CMAQ_{TOT}$ simulation. This is in agreement with prior studies (Han et al., 2015; Stavrakou et al., 2013; Vinken et al., 2014; Yegorova et al., 2011).

The production of HNO_3 from the reaction of $NO + HO_2$ (Butkovslaya et al., 2007) would lead to a decrease in NO_2. This channel of the $NO + HO_2$ reaction is not included in the CB05 chemical mechanism. Inclusion of this NO_x loss mechanism will have the largest impact in the tropics (Cariolle et al., 2008; Stavrakou et al., 2013). While changing the CB05 chemical mechanism may lead to better agreement between model output and satellite retrievals over the
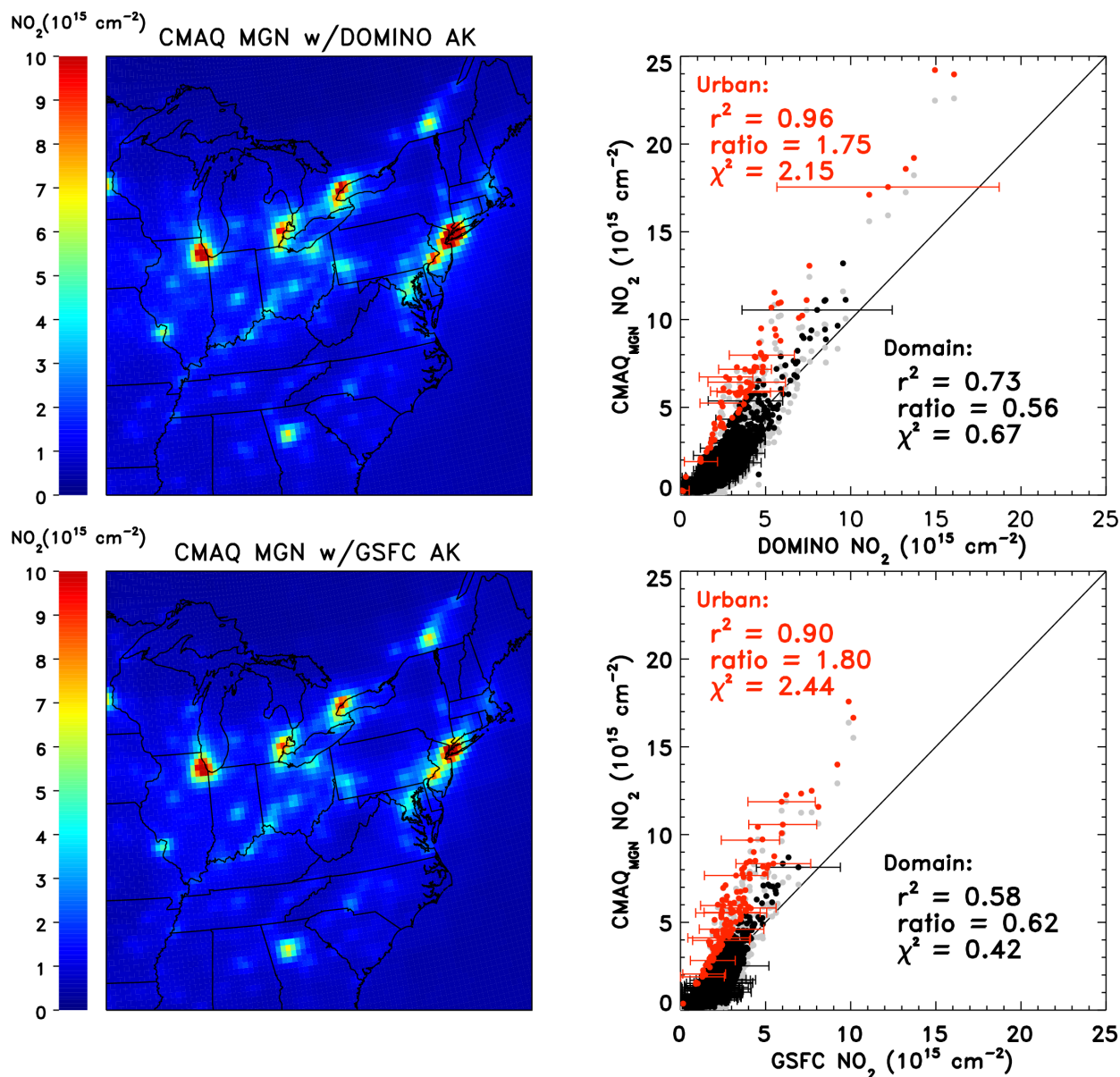
Figure 7. Same as Fig. 2 except model results include updated biogenic emissions from MEGANv2.10 (CMAQ$_{MGN}$). Gray points on the scatter plots represent the results shown in Fig. 2 (right panels).

urban regions described in this study, it would exacerbate the model/measurement discrepancy in rural areas.

Future work will investigate the importance of soil emissions of HONO, which are not included in the current versions of MEGAN and the chemical kinetics of other species that are important precursors to surface ozone. Prior studies indicate that soil emissions may account for 7 % of column NO$_2$ during the summer ozone season (Choi et al., 2008) and that HONO could be an important morning source of OH in an urban, VOC-rich environment (Ren et al., 2013).

6 Ozone

The focus of state implementation plans is attainment of the 8 h standard for surface ozone. It should be noted that CMAQ is most often used in a relative sense for this purpose. For instance, modifications to emissions inventories from a wide variety of sources, which represent future conditions based on possible proposed regulations, are run through CMAQ. Output from this model is compared to a base scenario to determine how much surface ozone is expected to decrease if these policy measures were to be enacted. For this study, we instead focus on the ability of CMAQ to reproduce ob-
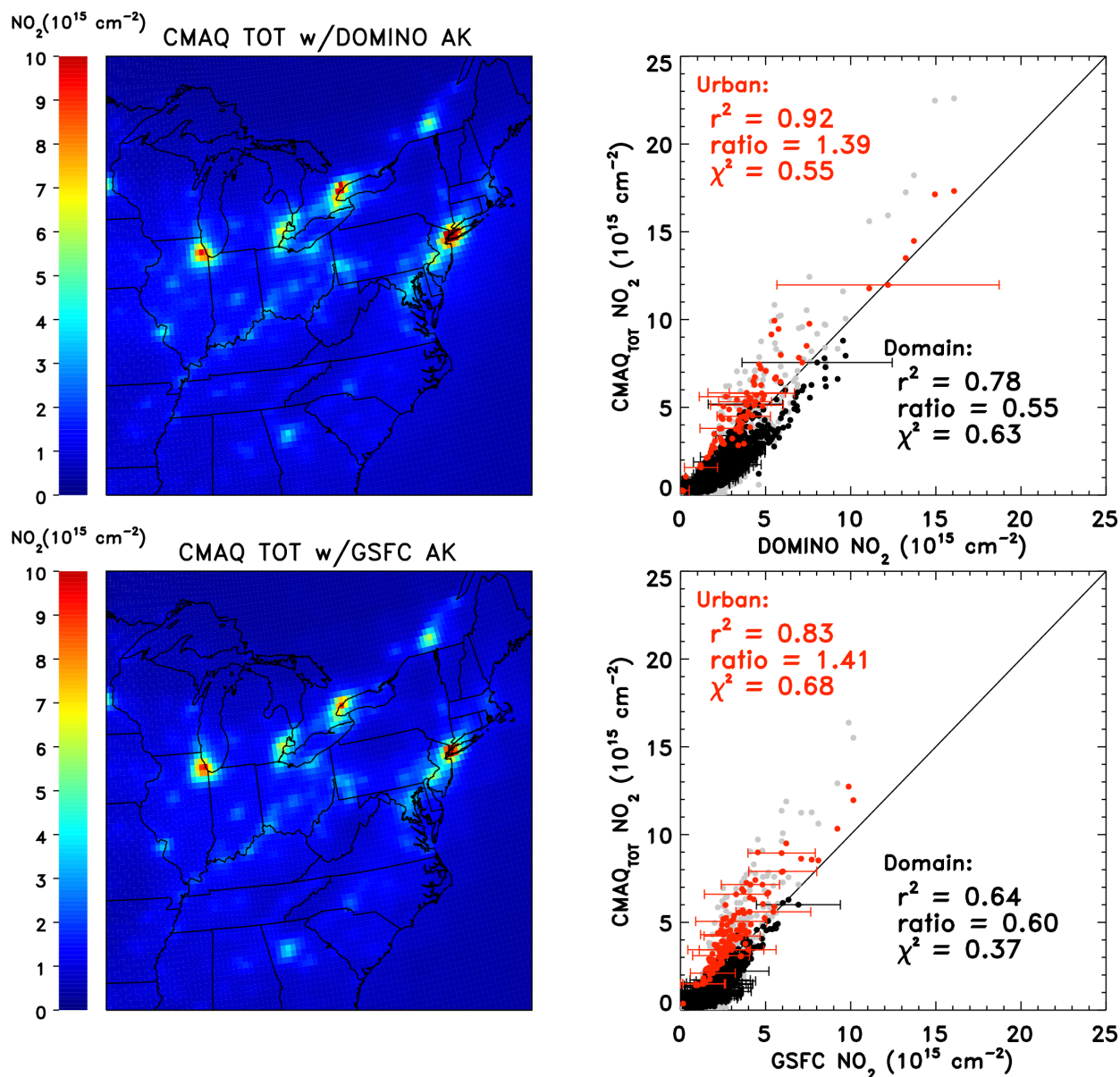
Figure 8. Same as Fig. 2 except model results include changes to NTR chemistry, a 50 % reduction in the emissions of NO$_x$ from mobile sources, and updated biogenic emissions (CMAQ$_{TOT}$). Gray points on the scatter plots represent the results shown in Fig. 2 (right panels).

served surface ozone. In Fig. 9, we compare average maximum daily 8 h average ozone from the four modeling scenarios considered above (CMAQ$_{BSE}$, CMAQ$_{NTR}$, CMAQ$_{N50}$, and CMAQ$_{TOT}$) to measured surface ozone from ground-based air quality observing sites (AQS). We have chosen to show the average of the daily maximum 8 h ozone for July and August 2007 at each model grid point. While it may seem that there were no violations of the 75 ppb standard, based on the scatter plots of model and observed ozone (Fig. 9, bottom), this is certainly not the case. There were exceedances of the 75 ppb ozone standard during this time; however, we have averaged these events with days having lower ozone.

There were no locations where the 62-day average of daily maximum 8 h ozone exceeded 75 ppb for this time period. An additional comparison, shown at the end of this section, will focus on days when the surface ozone standard was exceeded in Maryland.

All of the CMAQ simulations presented in Fig. 9 generally overestimate observed surface ozone. Ozone from CMAQ$_{BSE}$ is 26 % greater than observed (ratio of 1.26 denoted on Fig. 9), with 87 locations averaging higher than 75 ppb within the model. CMAQ results for CMAQ$_{NTR}$ lead to a further increase (32 %) in modeled ozone (an ozone disbenefit from this model change). While the changes made to
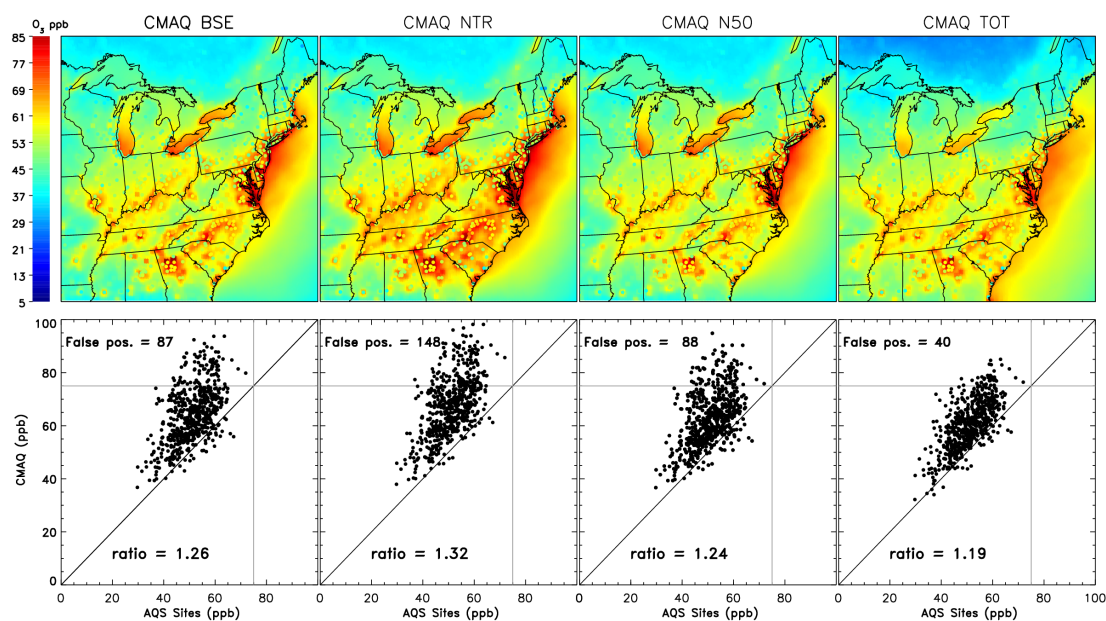
Figure 9. Average daily maximum 8 h daily ozone for July and August 2007 for four model cases: CMAQ$_{BSE}$ (top left), CMAQ$_{NTR}$ (top middle left), CMAQ$_{N50}$ (top middle right), and CMAQ$_{TOT}$ (top right) and ground based observations. Colored contours represent the CMAQ model output. Colored points denote average daily maximum 8 h daily ozone from ground-based AQS sites for the same time period. Scatter plots of each CMAQ model output vs. observations are shown (bottom panels). Gray horizontal and vertical lines indicate the 75 ppb ozone exceedance level. The number of times the model output is greater than 75 ppb while the observations are less than 75 ppb is shown (false positive). The mean ratio between CMAQ surface ozone and observations at air quality sites is indicated for each model simulation.

CB05 for CMAQ$_{NTR}$ provide a much more realistic representation of NO$_x$ chemistry (see Fig. 4), comparison of ozone found using CMAQ$_{NTR}$ and the baseline run suggests the presence of compensating errors in the chemistry and/or dynamics that control ozone. The inclusion of a 50 % reduction of mobile NO$_x$ (CMAQ$_{N50}$) (Anderson et al., 2014) leads to a decrease in modeled ozone compared to results from the CMAQ$_{NTR}$ run. Simulated ozone is still 24 % greater than measured, although there is slight improvement compared to the baseline run. Improved agreement between model and AQS observations of ozone occurs when updated biogenic emissions are also included, together with the aforementioned changes to mobile NO$_x$ and the lifetime of NTR. In this scenario, CMAQ$_{TOT}$, the model/measurement discrepancy for ozone is reduced to 19 % and there are only 40 false positives. The reason for this model behavior is that the reduction in isoprene emission upon use of MEGANv2.10 leads to decreases in HO$_2$ and RO$_2$, important ozone precursors.

If a ground-based ozone monitor reports 8 h average ozone exceeding the NAAQS standard, currently 75 ppb, it is considered to be in non-attainment. These sites are the subject of intense focus by state agencies to determine the fundamental causes of the ozone exceedance (e.g., local sources of pollution vs. out of state upwind sources). A comparison of ozone on days when observed ozone exceeded 75 ppb in Maryland during July and August 2007

to CMAQ model output is shown in Fig. 10. It should be noted that the ozone standard in 2007 was 80 ppb. However, the state of Maryland provides historic ozone data for the current, 75 ppb standard. These data can be found at https://data.maryland.gov/Energy-and-Environment/ Maryland-Ozone-Exceedance-Days-in-2007/iyzm-8pqd.

The model values of daily 8 h average ozone represent the closest points, spatially, to the monitor sites on the day that the exceedance occurred. For all model cases, CMAQ shows greater variability than the ground-based monitors during times of ozone exceedance. The overall analysis of the model runs for these days/times leads to results similar to the analysis in Fig. 9. The decrease in the lifetime of NTR (13 % overestimate) leads to an increase in model ozone compared to baseline (6 % overestimate), while the model that considers both reduced NTR lifetime and a 50 % decrease in mobile NO$_x$ emission yields an improved representation (2 % overestimate) of ozone compared to the baseline. Best agreement between modeled and observed ozone, for the times and place of exceedance, occurs when MEGANv.2.10 is considered along with the other model modifications. While the comparison still exhibits significant scatter about the 1 : 1 line, CMAQ is now on average in agreement with observed surface ozone (ratio of 1.00). This represents significant progress for the modeling of surface ozone, since we have prescribed a scenario for which the
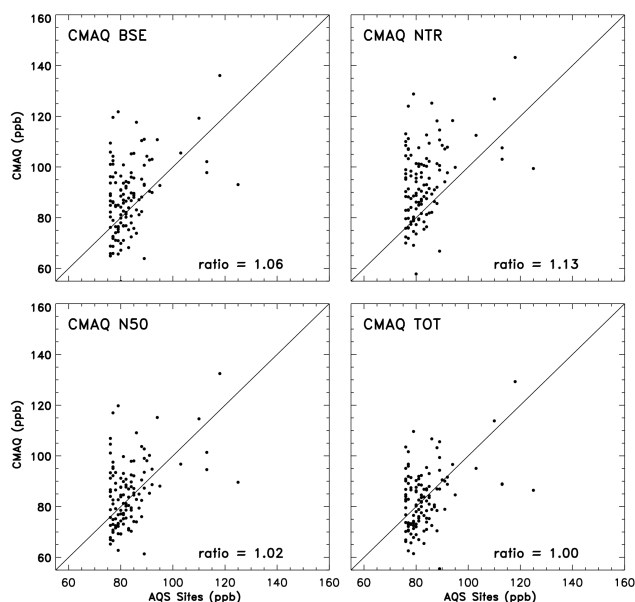
Figure 10. Comparison of average 8 h surface ozone calculated from baseline CMAQ model output (top left), CMAQ$_{NTR}$ model output (top right), CMAQ$_{N50}$ model output (bottom left panel), and CMAQ$_{TOT}$ (bottom right) to observations from ground-based AQS sites for those days and locations in Maryland that experienced exceedances (8 h average ozone greater than 75 ppb) during July and August 2007.

CMAQ air quality model is unbiased during a period of air quality exceedance.

7 Conclusions

We examine the ability of CMAQ to simulate reactive nitrogen over the eastern US by comparing model output to column content NO$_2$ observed by the OMI instrument on the AURA satellite. For July and August 2007, CMAQ consistently overestimates NO$_2$ over urban areas and underestimates NO$_2$ over rural areas relative to OMI observations; this finding is insensitive to the choice of GSFC or DOMINO retrieval product. Neither inclusion of lightning NO$_x$ nor consideration of the averaging kernel/scattering weights for OMI alters this conclusion. While the absolute value of NO$_2$ column content is subject to errors from a variety of sources, the urban / rural ratio provides a rigorous test of CMAQ's ability to simulate the photochemistry of NO$_2$ and the transport of this important criteria air pollutant. Because CMAQ using the CB05 mechanism overestimates the urban to rural ratio of tropospheric column NO$_2$, this model may underestimate the interstate transport of NO$_x$ and/or NO$_x$ reservoirs.

The CB05 chemical mechanism represents all alkyl nitrates as isopropyl nitrate – a reasonable simplification given the state of knowledge at the time of creation. However, there is now substantial evidence of a larger variety of alkyl ni-

trates and substituted alkyl nitrates (Horowitz et al., 2007; Perring et al., 2009; Beaver et al., 2012). These can have lifetimes as short as hours and recycle NO$_x$ much faster than short chain alkyl nitrates. Reducing the simulated lifetime of NTR in CB05 from $\sim$ 10 days to $\sim$ 1 day improves the agreement between measured and modeled tropospheric column NO$_2$ for the Baltimore–Washington area. This modification to CB05 reduces, but does not eliminate the urban / rural NO$_2$ bias within CMAQ. Implementation of a factor of 2 reduction in NO$_x$ emissions from mobile sources, based on Anderson et al. (2014) and analysis of ground-based observations for summer 2007, decreases NO$_2$ in urban regions that have a high-density of vehicular traffic, which improves the CMAQ representation of the ratio of urban to rural NO$_2$. Use of the latest MEGAN emissions for VOCs, v2.10 (Guenther et al., 2012), increases NO$_2$ throughout the domain and further improves the CMAQ representation of urban to rural NO$_2$, due to smaller levels of RO$_2$. The reduction in isoprene, which leads to the decrease in RO$_2$, is caused by the diminished sensitivity of isoprene emissions to PAR in the newer version of MEGAN.

We have also examined the effect of these various model runs on the CMAQ representation of surface ozone. Reducing the lifetime of NTR by a factor of 10 increases the average daily 8 h maximum ozone by $\sim$ 5 %; decreasing mobile source NO$_x$ emissions by a factor of 2 decreases ozone by about 6 %. The use of MEGAN v2.10 causes surface ozone to fall by 2.5 % relative to a simulation that is identical, except for use of MEGAN 2.04. Combining all three of these model changes (i.e., factor of 10 reduction in NTR lifetime, factor of 2 reduction in mobile NO$_x$, MEGAN v2.10) leads to the best simulation of surface ozone for the mid-Atlantic. This model run leads to agreement with the 2-month average of daily 8 h maximum ozone at the $\pm$20 % level, fewest number of false positives of an ozone exceedance throughout the domain, as well as an unbiased simulation of surface ozone at ground-based AQS sites that experienced an ozone exceedance (8 h ozone greater than 75 ppb) within Maryland during July and August 2007. The prescription of an unbiased simulation of ozone, coupled with a fairly accurate simulation of the urban to rural ratio of column NO$_2$, may provide a framework for use in studies focused on achieving future adherence to specific air quality standards for surface ozone by reducing emission of NO$_x$ from various anthropogenic sectors.

The Supplement related to this article is available online at doi:10.5194/acp-15-10965-2015-supplement.

Edited by: C. H. Song

References

Acarreta, J. R., De Haan, J. F., and Stamnes, P.: Cloud pressure retrieval using the O$_2$–O$_2$ absorption band at 477 nm, J. Geophys. Res., 109, D05204, doi:10.1029/2003JD003915, 2004.

Allen, D. J., Pickering, K. E., Pinder, R. W., Henderson, B. H., Appel, K. W., and Prados, A.: Impact of lightning-NO on eastern United States photochemistry during the summer of 2006 as determined using the CMAQ model, Atmos. Chem. Phys., 12, 1737–1758, doi:10.5194/acp-12-1737-2012, 2012.

Anderson, D. C., Loughner, C. P., Weinheimer, A., Diskin, D., Canty, T. P., Salawitch, R. J., Worden, H., Freid, A., Mikoviny, T., Wisthaler, A., and Dickerson, R. R.: Measured and modeled CO and NO$_y$ in DISCOVER-AQ: an evaluation of emissions and chemistry over the eastern US, Atmos. Environ., 96, 78–87, 2014.

Atlas, E.: Evidence for greater than or equal to C$_3$ alkyl nitrates in rural and remote atmospheres, Nature, 331, 426–428, 1988.

Atkinson, R., Baulch, D. L., Cox, R. A., Crowley, J. N., Hampson, R. F., Hynes, R. G., Jenkin, M. E., Rossi, M. J., and Troe, J.: Evaluated kinetic and photochemical data for atmospheric chemistry: Volume I – gas phase reactions of O$_x$, HO$_x$, NO$_x$ and SO$_x$ species, Atmos. Chem. Phys., 4, 1461–1738, doi:10.5194/acp-4-1461-2004, 2004.

Beaver, M. R., Clair, J. M. St., Paulot, F., Spencer, K. M., Crounse, J. D., LaFranchi, B. W., Min, K. E., Pusede, S. E., Wooldridge, P. J., Schade, G. W., Park, C., Cohen, R. C., and Wennberg, P. O.: Importance of biogenic precursors to the budget of organic nitrates: observations of multifunctional organic nitrates by CIMS and TD-LIF during BEARPEX 2009, Atmos. Chem. Phys., 12, 5773–5785, doi:10.5194/acp-12-5773-2012, 2012.

Boccippio, D., Cummins, K., Christian, H., and Goodman, S.: Combined satellite- and surface-based estimation of the intra-cloud-to-ground lightning ratio over the continental United States, Mon. Weather Rev., 129, 108–122, 2001.

Boersma, K. F., Eskes, H. J., Veefkind, J. P., Brinksma, E. J., van der A, R. J., Sneep, M., van den Oord, G. H. J., Levelt, P. F., Stammes, P., Gleason, J. F., and Bucsela, E. J.: Near-real time retrieval of tropospheric NO$_2$ from OMI, Atmos. Chem. Phys., 7, 2103–2118, doi:10.5194/acp-7-2103-2007, 2007.

Boersma, K. F., Eskes, H. J., Dirksen, R. J., van der A, R. J., Veefkind, J. P., Stammes, P., Huijnen, V., Kleipool, Q. L., Sneep, M., Claas, J., Leitão, J., Richter, A., Zhou, Y., and Brunner, D.: An improved tropospheric NO$_2$ column retrieval algorithm for the Ozone Monitoring Instrument, Atmos. Meas. Tech., 4, 1905–1928, doi:10.5194/amt-4-1905-2011, 2011.

Brent, L. C., Thorn, W. J., Gupta, M., Leen, B., Stehr, J. W., He, H., Arkinson, H. L., Weinheimer, A., Garland, C., Pusede, S. E., Wooldridge, P. J., Cohen, R. C., and Dickerson, R. R.: Evaluation of the use of a commercially available cavity ringdown absorption spectrometer for measuring NO$_2$ in flight, and observations over the Mid-Atlantic States, during DISCOVER-AQ, J. Atmos. Chem., doi:10.1007/s10874-013-9265-6, 2013.

Bucsela, E. J., Krotkov, N. A., Celarier, E. A., Lamsal, L. N., Swartz, W. H., Bhartia, P. K., Boersma, K. F., Veefkind, J. P., Gleason, J. F., and Pickering, K. E.: A new stratospheric and tropospheric NO$_2$ retrieval algorithm for nadir-viewing satellite instruments: applications to OMI, Atmos. Meas. Tech., 6, 2607–2626, doi:10.5194/amt-6-2607-2013, 2013.

Butkovskaya, N. I., Kukui, A., and Le Bras, G.: HNO$_3$ forming channel of the HO$_2$ + NO reaction as a function of pressure and temperature in the ranges of 72–600 Torr and 223–323 K, J. Phys. Chem. A, 111, 9047–9053, 2007.

Butler, T. J., Vermeylen, F. M., Rury, M., Likens, G. E., Lee, B., Bowker, G. E., and McCluney, L.: Response of ozone and nitrate to stationary source NO$_x$ emission reductions in the eastern USA, Atmos. Environ., 45, 1084–1094, doi:10.1016/j.atmosenv.2010.11.040, 2011.

Byun, D. and Schere, K. L.: Review of the governing equations, computational algorithms, and other components of the models-3 Community Multiscale Air Quality (CMAQ) modeling system, Appl. Mech. Rev., 59, 51–77, 2006.

Carlton, A. G. and Baker, K.: Photochemical modeling of the Ozark isoprene volcano: MEGAN, BEIS, and their impacts on air quality predictions, Environ. Sci. Technol., 45, 4438–4445, doi:10.1021/es200050x, 2011.

Cariolle, D., Evans, M., Chipperfield, M., Butkovskaya, N., Kukui, A., and LeBras, G.: Impact of the new HNO$_3$–forming channel of the HO$_2$ + OH reaction on tropospheric HNO$_3$, NO$_x$, HO$_x$, and ozone, Atmos. Chem. Phys., 8, 4061–4068, doi:10.5194/acp-8-4061-2008, 2008.

Castellanos, P.: Analysis of Air Quality with Numerical Simulations (CMAQ), and Observations of Trace Gases, The University of Maryland, College Park, 168 pp., 2009.

Castellanos, P., Marufu, L. T., Doddridge, B. G., Taubman, B. F., Schwab, J. J., Hains, J. C., Ehrman, S. H., and Dickerson, R. R.: Ozone, oxides of nitrogen, and carbon monoxide during pollution events over the eastern United States: an evaluation of emissions and vertical mixing, J. Geophys. Res., 116, D16307, doi:10.1029/2010JD014540, 2011.

Choi, Y., Wang, Y., Zeng, T., Cunnold, D., Yang, E.-S., Martin, R., Chance., K., Thouret, V., and Edgerson, E.: Springtime transitions of NO$_2$, CO, and O$_3$ over North America: model evaluation and analysis, J. Geophys. Res., 113, D20311, doi:10.1029/2007JD009632, 2008.

Day, D. A., Dillon, M. B., Wooldridge, P. J., Thornton, J. A., Rosen, R. S., Wood, E. C., and Cohen, R. C.: On alkyl nitrates, O$_3$, and the "missing NO$_y$", J. Geophys. Res., 108, 4501, doi:10.1029/2003JD003685, 2003.

Doraiswamy, P., Hogrefe, C., Hao, W., Henry, R. F., Civerolo, K., Ku, J.-Y., Sistla, G., Schwab, J. J., and Demerjian, K. L.: A diagnostic comparison of measured and model-predicted speciated VOC concentrations, Atmos. Environ., 43, 5759–5770, doi:10.1016/j.atmosenv.2009.07.056, 2009.

Duncan, B. N., Yoshida, Y., Olson, J. R., Sillman, S., Martin, R. V., Lamsal, L., Hu, Y., Pickering, K. E., Retscher, C., Allen, D. J., and Crawford, J. H.: Application of OMI observations to a space-based indicator of NO$_x$ and VOC controls on surface ozone formation, Atmos. Environ., 44, 2213–2223, 2010.

Dunlea, E. J., Herndon, S. C., Nelson, D. D., Volkamer, R. M., San Martini, F., Sheehy, P. M., Zahniser, M. S., Shorter, J. H., Wormhoudt, J. C., Lamb, B. K., Allwine, E. J., Gaffney, J. S., Marley, N. A., Grutter, M., Marquez, C., Blanco, S., Cardenas, B., Retama, A., Ramos Villegas, C. R., Kolb, C. E., Molina, L. T., and Molina, M. J.: Evaluation of nitrogen dioxide chemiluminescence monitors in a polluted urban environment, Atmos. Chem. Phys., 7, 2691–2704, doi:10.5194/acp-7-2691-2007, 2007.

EPA v. EME: Homer City Generation, 12–1183, US, 11–1302, 2014.

Farmer, D. K., Wooldridge, P. J., and Cohen, R. C.: Application of thermal-dissociation laser induced fluorescence (TD-LIF) to measurement of HNO$_3$, Σalkyl nitrates, Σperoxy nitrates, and NO$_2$ fluxes using eddy covariance, Atmos. Chem. Phys., 6, 3471–3486, doi:10.5194/acp-6-3471-2006, 2006.

Fehsenfeld, F. C., Dickerson, R. R., Hubler, G., Luke, W. T., Nunnermacker, L. J., Williams, E. J., Roberts, J. M., Calvert, J. G., Curran, C. M., Delany, A. C., Eubank, C. S., Fahey, D. W., Fried, A., Gandrud, B. W., Langford, A. O., Murphy, P. C., Norton, R. B., Pickering, K. E., and Ridley, B. A.: A Ground-Based Intercomparison of NO, NO$_x$, and NO$_y$ Measurement Techniques, J. Geophys. Res., 92, 14710–14722, 1987.

Fiore, A. M., Jacob, D. J., Logan, J. A., and Yin, J. H.: Long-term trends in ground level ozone over the contiguous United States, 1980–1995, J. Geophys. Res., 103, 1471–1480, 1998.

Flynn, C. M., Pickering, K. E., Crawford, J. H., Lamsal, L. N., Krotkov, N. A., Herman, J., Weinheimer, A., Chen, G., Liu, X., Szykman, J., Tsay, S. C., Laughner, C. P., Hains, J., Lee, P., Dickerson, R. R., Stehr, J. W., and Brent, L.: The relationship between column-density and surface mixing ratio: statistical analysis of O$_3$ and NO$_2$ data from the July 2011 Maryland DISCOVER-AQ mission, Atmos. Environ., 92, 429–441, 2014.

Fujita, E. M., Campbell, D. E., Stockwell, W. R., and Lawson, D. R.: Past and future ozone trends in California's South Coast Air Basin: reconciliation of ambient measurements with past and projected emission inventories, J. Air Waste Manage., 63, 54–69, 2013.

Gego, E., Porter, P. S., Gilliland, A., and Rao, S. T.: Observation-based assessment of the impact of nitrogen oxides emissions reductions on ozone air quality over the eastern United States, J. Appl. Meteorol. Clim., 46, 994–1008, 2007.

Gilliland, A. B., Hogrefe, C., Pinder, R. W., Godowitch, J. M., Foley, K. L., and Rao, S. T.: Dynamic evaluation of regional air quality models: assessing changes in O$_3$ stemming from changes in emissions and meteorology, Atmos. Environ., 42, 5110–5123, 2008.

Godowitch, J. M., Hogrefe, C., and Rao, S. T.: Diagnostic analyses of a regional air quality model: changes in modeled processes affecting ozone and chemical-transport indicators from NO$_x$ point source emission reductions, J. Geophys. Res., 113, D19303, doi:10.1029/2007JD009537, 2008a.

Godowitch, J. M., Gilliland, A. B., Draxler, R. R., and Rao, S. T.: Modeling assessment of point source NO$_x$ emission reductions on ozone air quality in the eastern United States, Atmos. Environ., 42, 87–100, 2008b.

Goldberg, D. L., Loughner, C. P., Tzortziou, M., Stehr, J. W., Pickering, K. E., Marufu, L. T., and Dickerson, R. R.: Higher surface ozone concentrations over the Chesapeake Bay than over the ad-

jacent land: observations and models from the DISCOVER-AQ and CBODAQ campaigns, Atmos. Environ., 84, 9–19, 2014.

Guenther, A., Karl, T., Harley, P., Wiedinmyer, C., Palmer, P. I., and Geron, C.: Estimates of global terrestrial isoprene emissions using MEGAN (Model of Emissions of Gases and Aerosols from Nature), Atmos. Chem. Phys., 6, 3181–3210, doi:10.5194/acp-6-3181-2006, 2006.

Guenther, A. B., Jiang, X., Heald, C. L., Sakulyanontvittaya, T., Duhl, T., Emmons, L. K., and Wang, X.: The Model of Emissions of Gases and Aerosols from Nature version 2.1 (MEGAN2.1): an extended and updated framework for modeling biogenic emissions, Geosci. Model Dev., 5, 1471–1492, doi:10.5194/gmd-5-1471-2012, 2012.

Hains, J. C., Taubman, B. F., Thompson, A. M., Stehr, J. W., Marufu, L. T., Doddridge, B. G., and Dickerson, R. R.: Origins of chemical pollution derived from Mid-Atlantic aircraft profiles using a clustering technique, Atmos. Environ., 42, 1727–1741, 2008.

Han, K. M., Lee, S., Chang, L. S., and Song, C. H.: A comparison study between CMAQ-simulated and OMI-retrieved NO$_2$ columns over East Asia for evaluation of NO$_x$ emission fluxes of INTEX–B, CAPSS, and REAS inventories, Atmos. Chem. Phys., 15, 1913–1938, doi:10.5194/acp-15-1913-2015, 2015.

He, H., Hembeck, L., Hosley, K. M., Canty, T. P., Salawitch, R. J., and Dickerson, R. R.: High ozone concentrations on hot days: the role of electric power demand and NO$_x$ emissions, Geophys. Res. Lett., 40, 5291–5294, 2013a.

He, H., Stehr, J. W., Hains, J. C., Krask, D. J., Doddridge, B. G., Vinnikov, K. Y., Canty, T. P., Hosley, K. M., Salawitch, R. J., Worden, H. M., and Dickerson, R. R.: Trends in emissions and concentrations of air pollutants in the lower troposphere in the Baltimore/Washington airshed from 1997 to 2011, Atmos. Chem. Phys., 13, 7859–7874, doi:10.5194/acp-13-7859-2013, 2013b.

He, H., Loughner, C. P., Stehr, J. W., Arkinson, H. L. Brent, L. C., Follette-Cook, M. B., Tzortziou, M. A. Pickering, K. E., Thompson, A. M., Martins, D. K., Diskin, G. S., Anderson, B. E., Crawford, J. H., Weinheimer, A. J., Lee, P., Hains, J. C., and Dickerson, R. R.: An elevated reservoir of air pollutants over the Mid-Atlantic States during the 2011 DISCOVER-AQ campaign: airborne measurements and numerical simulations, Atmos. Environ., 85, 18–30, doi:10.1016/j.atmosenv.2013.11.039, 2014.

Hogrefe, C., Isukapalli, S. S., Tang, X. G., Georgopoulos, P. G., He, S., Zalewsky, E. E., Hao, W., Ku, J. Y., Key, T., and Sistla, G.: Impact of biogenic emission uncertainties on the simulated response of ozone and fine particulate matter to anthropogenic emission reductions, J. Air Waste Manage., 61, 92–108, 2011.

Horowitz, L. W., Fiore, A. M., Milly, G. P., Cohen, R. C., Perring, A., Wooldridge, P. J., Hess, P. G., Emmons, L. K., and Lamarque, J.: Observational constraints on the chemistry of isoprene nitrates over the eastern United States, J. Geophys. Res., 112, D12S08, doi:10.1029/2006JD007747, 2007.

Jacobson, M. Z., Wilkerson, J. T., Naiman, A. D., and Lele, S. K.: The effects of aircraft on climate and pollution. Part II: 20-year impacts of exhaust from all commercial aircraft worldwide treated individually at the subgrid scale, Faraday Discuss., 165, 369–381, 2013.

Lamsal, L. N., Krotkov, N. A., Celarier, E. A., Swartz, W. H., Pickering, K. E., Bucsela, E. J., Gleason, J. F., Martin, R. V.,

Philip, S., Irie, H., Cede, A., Herman, J., Weinheimer, A., Szykman, J. J., and Knepp, T. N.: Evaluation of OMI operational standard NO$_2$ column retrievals using in situ and surface-based NO$_2$ observations, Atmos. Chem. Phys., 14, 11587–11609, doi:10.5194/acp-14-11587-2014, 2014.

Leucken, D. and Schwede, D.: Improving the treatment of oxidized nitrogen in CMAQ influence of gas phase chemical and physical parameterizations, talk presented at: Community Modeling and Analysis System conference, Friday Center, UNC-Chapel Hill, USA, 2014.

Li, G., Zhang, R., Fan, J., and Tie, X.: Impacts of biogenic emissions on photochemical ozone production in Houston, Texas, J. Geophys. Res., 112, D10309, doi:10.1029/2006JD007924, 2007.

Lockwood, A. L., Shepson, P. B., Fiddler, M. N., and Alaghmand, M.: Isoprene nitrates: preparation, separation, identification, yields, and atmospheric chemistry, Atmos. Chem. Phys., 10, 6169–6178, doi:10.5194/acp-10-6169-2010, 2010.

Logan, J. A.: Ozone in rural-areas of the United States, J. Geophys. Res., 94, 8511–8532, 1989.

Loughner, C. P., Allen, D. J., Pickering, K. E., Zhang, D. L., Shou, Y. X., and Dickerson, R. R.: Impact of fair-weather cumulus clouds and the Chesapeake Bay breeze on pollutant transport and transformation, Atmos. Environ., 45, 4060–4072, 2011.

Luke, W. T., Dickerson, R. R., and Nunnermacker, L. J.: Direct measurements of the photolysis rate coefficients and Henry Law constants of several alkyl nitrates, J. Geophys. Res., 94, 14905–14921, 1989.

Marufu, L. T., Taubman, B. F., Bloomer, B., Piety, C. A., Doddridge, B. G., Stehr, J. W., and Dickerson, R. R.: The 2003 North American electrical blackout: an accidental experiment in atmospheric chemistry, Geophys. Res. Lett., 31, L13106, doi:10.1029/2004GL019771, 2004.

Mollner, A. K., Valluvadasan, S., Feng, L., Sprague, M. K., Okumura, M., Milligan, D. B., Bloss, W. J., Sander, S. P., Martien, P. T., Harley, R. A., McCoy, A. B., and Carter, W. P. L.: Rate of Gas Phase Association of Hydroxyl Radical and Nitrogen Dioxide, Science, 330, 646–649, doi:10.1126/science.1193030, 2010.

Müller, J.-F., Peeters, J., and Stavrakou, T.: Fast photolysis of carbonyl nitrates from isoprene, Atmos. Chem. Phys., 14, 2497–2508, doi:10.5194/acp-14-2497-2014, 2014.

Napelenok, S. L., Pinder, R. W., Gilliland, A. B., and Martin, R. V.: A method for evaluating spatially-resolved NO$_x$ emissions using Kalman filter inversion, direct sensitivities, and space-based NO$_2$ observations, Atmos. Chem. Phys., 8, 5603–5614, doi:10.5194/acp-8-5603-2008, 2008.

Neff, J., Holland, E., Dentener, F., McDowell, W., and Russell, K.: The origin, composition and rates of organic nitrogen deposition: a missing piece of the nitrogen cycle?, Biogeochemistry, 57–58, 99–136, 2002.

Paulot, F., Crounse, J. D., Kjaergaard, H. G., Kroll, J. H., Seinfeld, J. H., and Wennberg, P. O.: Isoprene photooxidation: new insights into the production of acids and organic nitrates, Atmos. Chem. Phys., 9, 1479–1501, doi:10.5194/acp-9-1479-2009, 2009.

Perring, A. E., Bertram, T. H., Wooldridge, P. J., Fried, A., Heikes, B. G., Dibb, J., Crounse, J. D., Wennberg, P. O., Blake, N. J., Blake, D. R., Brune, W. H., Singh, H. B., and Cohen, R. C.: Airborne observations of total RONO$_2$: new constraints on the yield and lifetime of isoprene nitrates, Atmos. Chem. Phys., 9, 1451–1463, doi:10.5194/acp-9-1451-2009, 2009.

Perring, A. E., Bertram, T. H., Farmer, D. K., Wooldridge, P. J., Dibb, J., Blake, N. J., Blake, D. R., Singh, H. B., Fuelberg, H., Diskin, G., Sachse, G., and Cohen, R. C.: The production and persistence of ΣRONO$_2$ in the Mexico City plume, Atmos. Chem. Phys., 10, 7215–7229, doi:10.5194/acp-10-7215-2010, 2010.

Perring, A. E., Pusede, S. E., and Cohen, R. C.: An observational perspective on the atmospheric impacts of alkyl and multifunctional nitrates on ozone and secondary organic aerosol, Chem. Rev., 113, 5848–5870, doi:10.1021/cr300520x, 2013.

Pollack, I. B., Ryerson, T. B., Trainer, M., Neuman, J. A., Roberts, J. M., and Parrish, D. D.: Trends in ozone, its precursors, and related secondary oxidation products in Los Angeles, California: a synthesis of measurements from 1960 to 2010, J. Geophys. Res., 118, 5893–5911, 2013.

Ren, X., Van Duin, D., Cazorla, M., Chen, S., Brune, W. H., Flynn, J. H., Grossberg, N., Lefer, B. L., Rappengluck, B., Wong, K. W., Tsai, C., Stutz, J., Dibb, J. E., Jobson, B. T., Luke, W., and Kelley, P.: Atmospheric oxidation chemistry and ozone production: results from SHARP 2009 in Houston, Texas, J. Geophys. Res., 118, 5770–5780, doi:10.1002/jgrd.50342, 2103.

Russell, A. R., Perring, A. E., Valin, L.'C., Bucsela, E. J., Browne, E. C., Wooldridge, P. J., and Cohen, R. C.: A high spatial resolution retrieval of NO$_2$ column densities from OMI: method and evaluation, Atmos. Chem. Phys., 11, 8543–8554, doi:10.5194/acp-11-8543-2011, 2011.

Ryan, W. F., Doddridge, B. G., Dickerson, R. R., Morales, R. M., Hallock, K. A., Roberts, P. T., Blumenthal, D. L., Anderson, J. A., and Civerolo, K. L.: Pollutant transport during a regional O$_3$ episode in the mid-Atlantic states, J. Air Waste Manage., 48, 786–797, 1998.

Sander, S. P. , Friedl, R. R., Golden, D. M., Kurylo, M. J., Moortgat, G. K., Keller-Rudek, H., Wine, P. H., Ravishankara, A. R., Kolb, C. E., Molina, M. J., Finlayson-Pitts, B. J., Huie, R. E., and Orkin, V. L.: Chemical Kinetics and Photochemical Data for Use in Atmospheric Studies, JPL Publication 06-2, Evaluation no. 15, 2006.

Stavrakou, T., Müller, J.-F., Boersma, K. F., van der A, R. J., Kurokawa, J., Ohara, T., and Zhang, Q.: Key chemical NO$_x$ sink uncertainties and how they influence top-down emissions of nitrogen oxides, Atmos. Chem. Phys., 13, 9057–9082, doi:10.5194/acp-13-9057-2013, 2013.

Taubman, B. F., Marufu, L. T., Piety, C. A., Doddridge, B. G., Stehr, J. W., and Dickerson, R. R.: Airborne characterization of the chemical, optical, and meteorological properties, and origins of a combined ozone/haze episode over the eastern US, J. Atmos. Sci., 61, 1781–1793, 2004.

Taubman, B. F., Hains, J. C., Thompson, A. M., Marufu, L. T., Doddridge, B. G., Stehr, J. W., Piety, C. A., and Dickerson, R. R.: Aircraft vertical profiles of trace gas and aerosol pollution over the mid-Atlantic United States: statistics and meteorological cluster analysis, J. Geophys. Res., 111, D10S07, doi:10.1029/2005JD006196, 2006.

USEPA (United States Environmental Protection Agency): EPA's National Inventory Model (NMIM), A Consolidated Emissions

Modeling System for MOBILE6 and NONROAD, Office of Transportation and Air Quality, EPA420-B-09-015, 2005.

USEPA (United States Environmental Protection Agency): Technical Guidance on the Use of MOVES2010 for Emission Inventory Preparation in State Implementation Plans and Transportation Conformity, EPA-420-B-10-023, 2010.

van Noije, T. P. C., Eskes, H. J., Dentener, F. J., Stevenson, D. S., Ellingsen, K., Schultz, M. G., Wild, O., Amann, M., Atherton, C. S., Bergmann, D. J., Bey, I., Boersma, K. F., Butler, T., Cofala, J., Drevet, J., Fiore, A. M., Gauss, M., Hauglustaine, D. A., Horowitz, L. W., Isaksen, I. S. A., Krol, M. C., Lamarque, J. F., Lawrence, M. G., Martin, R. V., Montanaro, V., Muller, J. F., Pitari, G., Prather, M. J., Pyle, J. A., Richter, A., Rodriguez, J. M., Savage, N. H., Strahan, S. E., Sudo, K., Szopa, S., and van Roozendael, M.: Multi-model ensemble simulations of tropospheric NO$_2$ compared with GOME retrievals for the year 2000, Atmos. Chem. Phys., 6, 2943–2979, 2006, doi:10.5194/acp-6-2943-2006, 2006.

Vinken, G. C. M., Boersma, K. F., van Donkelaar, A., and Zhang, L.: Constraints on ship NO$_x$ emissions in Europe using GEOS–Chem and OMI satellite NO$_2$ observations, Atmos. Chem. Phys., 14, 1353–1369, doi:10.5194/acp-14-1353-2014, 2014.

Walsh, K. J., Milligan, M., Woodman, M., and Sherwell, J.: Data mining to characterize ozone behavior in Baltimore and Washington, DC, Atmos. Environ., 42, 4280–4292, 2008.

Wilson, R. C., Fleming, Z. L., Monks, P. S., Clain, G., Henne, S., Konovalov, I. B., Szopa, S., and Menut, L.: Have primary emission reduction measures reduced ozone across Europe? An analysis of European rural background ozone trends 1996–2005, Atmos. Chem. Phys., 12, 437–454, doi:10.5194/acp-12-437-2012, 2012.

Xie, Y., Paulot, F., Carter, W. P. L., Nolte, C. G., Luecken, D. J., Hutzell, W. T., Wennberg, P. O., Cohen, R. C., and Pinder, R. W.: Understanding the impact of recent advances in isoprene photooxidation on simulations of regional air quality, Atmos. Chem. Phys., 13, 8439–8455, doi:10.5194/acp-13-8439-2013, 2013.

Yarwood, G., Rao, S., Yocke, M., and Whitten, G. Z.: Updates to the Carbon Bond Chemical Mechanism: CB05, ENVIRON International Corp, 2005.

Yegorova, E. A., Allen, D. J., Loughner, C. P., Pickering, K. E., and Dickerson, R. R.: Characterization of an eastern US severe air pollution episode using WRF/Chem, J. Geophys. Res., 116, D17306, doi:10.1029/2010JD015054, 2011.

Yu, S., Mathur, R., Sarwar, G., Kang, D., Tong, D., Pouliot, G., and Pleim, J.: Eta-CMAQ air quality forecasts for O$_3$ and related species using three different photochemical mechanisms (CB4, CB05, SAPRC-99): comparisons with measurements during the 2004 ICARTT study, Atmos. Chem. Phys., 10, 3001–3025, doi:10.5194/acp-10-3001-2010, 2010.

Yu, S. C., Mathur, R. Pleim, J., Pouliot, G., Wong, D., Eder, B., Schere, K., Gilliam, R., and Rao, S. T.: Comparative evaluation of the impact of WRF-NMM and WRF-ARW meteorology on CMAQ simulations for O$_3$ and related species during the 2006 TexAQS/GoMACCS campaign, Atmos. Pollut. Res., 3, 149–162, doi:10.5094/APR.2012.015, 2012.

Zhou, W., Cohan, D. S., and Napelenok, S. L.: Reconciling NO$_x$ emissions reductions and ozone trends in the US, 2002–2006, Atmos. Environ., 70, 236–244, 2013.